

Electrical synapses connect a network of gonadotropin releasing hormone neurons in a cichlid fish

Yunyong Ma^{a,1}, Scott A. Juntti^{b,1}, Caroline K. Hu^b, John R. Huguenard^a, and Russell D. Fernald^{b,2}

^aDepartment of Neurology and Neurological Sciences, Stanford University School of Medicine, Stanford, CA 94305; and ^bDepartment of Biology, Stanford University, Stanford, CA 94305

Edited by Donald W. Pfaff, The Rockefeller University, New York, NY, and approved February 20, 2015 (received for review November 14, 2014)

Initiating and regulating vertebrate reproduction requires pulsatile release of gonadotropin-releasing hormone (GnRH1) from the hypothalamus. Coordinated GnRH1 release, not simply elevated absolute levels, effects the release of pituitary gonadotropins that drive steroid production in the gonads. However, the mechanisms underlying synchronization of GnRH1 neurons are unknown. Control of synchronicity by gap junctions between GnRH1 neurons has been proposed but not previously found. We recorded simultaneously from pairs of transgenically labeled GnRH1 neurons in adult male *Astatotilapia burtoni* cichlid fish. We report that GnRH1 neurons are strongly and uniformly interconnected by electrical synapses that can drive spiking in connected cells and can be reversibly blocked by meclofenamic acid. Our results suggest that electrical synapses could promote coordinated spike firing in a cellular assemblage of GnRH1 neurons to produce the pulsatile output necessary for activation of the pituitary and reproduction.

transgenic | GnRH | gap junction | cichlid | electrophysiology

Development and function of the reproductive system in vertebrates depends on the timing and levels of signaling by gonadal sex steroids (1, 2). Production of these steroids is controlled by neurons expressing gonadotropin-releasing hormone (GnRH1), which comprise the final output of the brain to the hypothalamic-pituitary-gonadal axis. During vertebrate development, GnRH1 neurons originate outside the central nervous system in the olfactory placode and migrate into the basal forebrain (3–6). These neurons signal to the pituitary via the decapeptide GnRH1 to effect the release of the gonadotropins, follicle stimulating hormone and luteinizing hormone, which in turn stimulate steroid production by the gonads. It has long been known that this release depends on coordinated, pulsatile GnRH1 release, not simply elevated levels (7, 8), requiring some level of synchronization in the output of these neurons. Episodic activation of the pituitary gonadotropes has been observed in multiple vertebrate taxa, including mammals and fish (9–12), however, mechanisms that underlie this required coordinated activity of GnRH1 neurons are unknown. Synchrony could in principle derive from coincident input from a “pacemaker” neural population, from direct coupling of GnRH1 neurons, or from a combination of mechanisms. Gap junction-mediated coupling has been suspected to play a role, as synchronous firing can be observed in neurons mechanically isolated from brain slices and in cultures of embryonic mouse and primate neurons, and immortalized mouse GnRH1 neurons express the connexin proteins that constitute gap junctions (13–15). However, no evidence for gap junctions among adult GnRH1 cells *in vivo* has been found (16, 17).

To search for the origin of synchrony among these neurons, we used a unique model system for analysis of GnRH1 neurons, *Astatotilapia burtoni*, a cichlid fish. GnRH1 neurons in males of this species exhibit dynamic morphological plasticity caused by changes in their social status (18–21). Here we use transgenic dominant male *A. burtoni* to perform paired recordings from GnRH1 neurons, and report that they are reciprocally connected by electrical synapses. These findings suggest that gap junctions contribute to the coordinated firing of these neurons necessary for reproductive function.

Results

We generated a transgenic *A. burtoni* line using *Tol2* transposase (22) and regulatory elements from the *GnRH1* locus to drive EGFP expression specifically in GnRH1 neurons (Fig. 1*A*). We observed green fluorescence in the transgenic brain only in cell bodies located in the preoptic area (POA), extending processes to the pituitary, hallmarks of GnRH1 neurons (Fig. 1*B*). We confirmed that these EGFP+ cells expressed GnRH1 by colabeling brain sections with antibodies against each and found that 98 ± 0.1% of GnRH1+ cells were also EGFP+, while 92 ± 0.2% of EGFP+ cells were GnRH1+ (Fig. 1 *C–F*; *n* = 3 fish). Our data show that transgenic *A. burtoni* can be used to systematically interrogate the connectivity of GnRH1 neurons with electrophysiological recordings.

We recorded simultaneously from 18 pairs of transgenically labeled GnRH1 neurons in the preoptic area from brain slices of reproductively active male *A. burtoni* and found that 17 of 18 pairs were electrically coupled (Fig. 2 *A–F*, Fig. S1, and Table S1). We used simultaneous current clamp to record responses of a GnRH1 neuron pair to steps of current injection. For coupled pairs of GnRH1 neurons, when we injected a depolarizing current into cell 1 while recording voltage from both cells, we observed a coupled depolarization plateau with action potential-correlated excitatory postsynaptic potentials (spikelets) riding on it in cell 2 (Fig. 2*G*; see also Fig. S1 *C–F*). In the reversed condition, depolarizing cell 2 while recording from both cells, symmetric electrical coupling was found from cell 2 to cell 1 (Fig. 2*H*). In both configurations, we observed action potentials in the stimulated cell and spikelets in the paired cell with a very short latency (Fig. 2 *G* and *H*), consistent with GnRH1 cells being coupled through gap junctions.

Significance

The hypothalamus controls reproductive development and function via a small peptide, gonadotropin releasing hormone (GnRH1), delivered to the pituitary. To be effective, GnRH1 must be released in a pulsatile manner, but it is not known how this is achieved. We recorded from pairs of genetically labeled GnRH1 neurons in the brains of reproductively active fish and show that these cells are strongly and uniformly interconnected by electrical synapses that can be reversibly blocked. These electrical synapses likely contribute to the pulsatile firing of GnRH1 neurons, producing the coordinated output needed for reproduction, the most important act of any organism.

Author contributions: Y.M., S.A.J., J.R.H., and R.D.F. designed research; Y.M. and S.A.J. performed research; C.K.H. contributed new reagents/analytic tools; Y.M., S.A.J., J.R.H., and R.D.F. analyzed data; and Y.M., S.A.J., J.R.H., and R.D.F. wrote the paper.

The authors declare no conflict of interest.

This article is a PNAS Direct Submission.

Freely available online through the PNAS open access option.

¹Y.M. and S.A.J. contributed equally to this work.

²To whom correspondence should be addressed. Email: rferald@stanford.edu.

This article contains supporting information online at www.pnas.org/lookup/suppl/doi:10.1073/pnas.1421851112/-DCSupplemental.

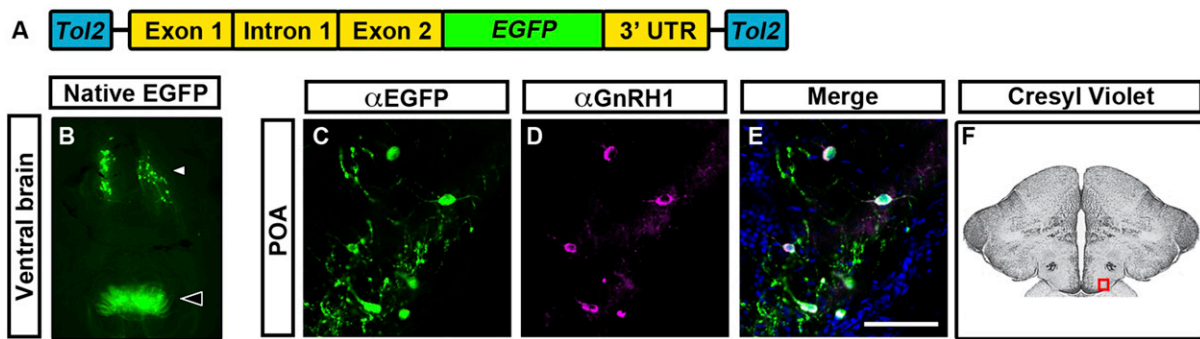


Fig. 1. *GnRH1:EGFP* transgene reliably marks GnRH1+ neurons. (A) Regulatory elements (yellow) from the endogenous *A. burtoni* *GnRH1* locus were used to drive EGFP expression. 5.8 kb of *GnRH1* noncoding sequence was fused to EGFP, and the construct was flanked by *Tol2* recognition sites. Not to scale. (B) Fish carrying the *GnRH1:EGFP* transgene exhibited robust green fluorescence at the ventral surface of the brain in cell bodies of the anterior hypothalamus (white arrowhead), fibers projecting posteriorly, and in the pituitary (open arrowhead). Up, anterior. (C–F) Cells in the POA coexpress EGFP (C) and GnRH1 (D) proteins. DAPI (blue in E) and cresyl violet (F) stained sections, with imaged area in C–E outlined in red, are shown for reference. (Scale bar, 50 μ m in C–E.)

To characterize the putative electrical connections, we used simultaneous current clamp to record responses of a GnRH1 neuron pair to steps of current injection. We held neurons with steady DC current at -60 to -67 mV, delivered depolarizing and hyperpolarizing current steps first into one GnRH1 neuron, and then into the other member of the pair. We observed mirror symmetric responses reflecting symmetry of the gap junction connections (Fig. 2 I and J). We calculated a coupling coefficient (CC) from cell 1 to cell 2 (CC_{1-2} ; ratio of V_m change in cell 2 to V_m change in cell 1 while injecting current into cell 1), and correspondingly for the reciprocal connection (CC_{2-1}) in 16 pairs (in one coupled pair, membrane potential fluctuations prevented the measurement). In 14 of the 16 pairs, the CC could be measured in both directions and we found no significant difference as a function of direction (Fig. 2 I and J; $CC_{1-2} = 0.14 \pm 0.02$ vs. $CC_{2-1} = 0.16 \pm 0.02$, $P = 0.23$, paired *t* test), suggesting that the gap junctions are electrically symmetric and produce neither rectification nor attenuation. There was no correlation between CC and either gonadosomatic index or intersomatic distance (Fig. 2 M and N). The measured values for CC are consistent with those reported from other neuronal types connected by gap junctions in vertebrate brains (23–27).

We also recorded occasional but strong, highly oscillatory, coordinated network coupling with multineuron input evident on each cycle of the oscillation (Fig. 3 A and B; Fig. S2, and Movie S1). We recorded simultaneously from 11 cell pairs in cell-attached voltage clamp mode in search of spontaneous spiking activity. Among the 22 individual cell recordings, more than half ($n = 13$ cells) were spontaneously active (1.21 ± 0.44 Hz mean spontaneous firing rate; range 0.01–4.6 Hz), consistent with previous recordings from single *A. burtoni* GnRH1 neurons (28). However, of the 11 pairs, only in 5 pairs were both cells spontaneously active. Of these, three (60%) had sufficiently numerous spikes to allow cross-correlations to be computed with confidence (Fig. 3B). The 8 pairs in which we could not ascribe synchrony had either infrequent spike firing that precluded statistical analysis, the activity observed was not composed of action potentials, or only one cell of the pair was active. Nevertheless, in each of the cases for which we observed robust, spontaneous firing in both cells, the cells exhibited coordinated spiking ($n = 3$ pairs). These coarsely synchronized, spontaneous action potentials were characteristic of being mediated via gap junctions. They revealed no reversal potential, as shown by the retention of polarity and magnitude of the network responses across large changes in postsynaptic membrane potential (Fig. S3). These results indicate that gap junction-mediated coordinated activity is a key feature of the GnRH1 system in *A. burtoni*.

We next asked whether gap junctions between GnRH1 neurons could facilitate coordinated spiking. We injected single 150-ms current pulses into two cells separately during paired recordings.

The amplitude of the single pulses was adjusted in each cell to be just subthreshold in the corresponding cells. This paradigm produced only small voltage deflections in the paired cell. However, when identical subthreshold current injections were delivered concurrently to both cells of the pair, there was an enhanced probability of spiking compared with temporally separated injections (Fig. 3 C and D). Thus, gap junction-mediated current transfer facilitates generation of action potentials across GnRH1 neurons.

Signal transmission through gap junctions is known to act as a low-pass filter (29). To assess this additional characteristic, we used a sine wave voltage command input (20 mV peak-to-peak) with increasing frequency (1–40 Hz in 2.5 s) and measured the coupling coefficient and phase shift as a function of frequency. The coupling coefficient decreased and the phase shift between input and output increased with increasing signal frequency (Fig. S4), with a 50% decrease in coupling coefficient, and a 60-degree phase lag at ~ 10 Hz. A decrease in coupling coefficient and phase shift with increased frequency is consistent with other reports of networks of electrically coupled neurons (29) and reflects typical low-pass filter circuit properties of neurons connected through gap junctions. Note that the pulsatile firing we observed in some slices (Fig. 3A and Fig. S2) was characterized by loose coordination, with multiple spikelets occurring during each cycle of pulsatile activity. Clusters of spikelets were coordinated within time windows of 50–100 ms, yielding slow ~ 1 - to 5-Hz waves of depolarization that would be subject to little or no signal attenuation (Fig. S4).

To assess the nature of the electrical coupling, we added known blockers of gap junctions to the slice perfusate. Octanol ($n = 2$), mefloquine ($n = 1$), and carbenoxolone ($n = 3$) were ineffective in altering electrical coupling. However, application of meclofenamic acid (400 μ M) (30, 31) resulted in the elimination of electrical conduction after ~ 15 –30 min (Fig. 4). After washing out the blocker for 45 min, conduction returned, further supporting the hypothesis that gap junctions mediate the coupling we observe among GnRH1 neurons.

We next asked whether GnRH1 neurons were electrically coupled with non-GnRH1 neurons. When recording from GnRH1 neurons and adjacent non-GnRH1 neurons, we found no detectable electrical coupling in either direction (Fig. 2 K and L; CC_{1-2} , $CC_{2-1} < 0.005$; $n = 3$ –4 pairs). This result suggests that gap junctions preferentially couple GnRH1 neurons to one another, but not to other adjacent cell types (17 of 18 GnRH1 to GnRH1 pairs; 0 of 4 GnRH1 to non-GnRH1 pairs; $P = 0.0007$, Fisher's exact test). Thus, the electrical coupling between GnRH1 neurons likely facilitates coordination of firing only within this population of neurons.

The electrical coupling we observe between GnRH1 neurons predicts that these neurons express connexins, the proteins that comprise gap junctions. We searched the *A. burtoni* genome for likely connexin genes, and focused on the neuronal connexin gap junction delta 2 (*Gjd2*; also known as Cx36 in mammals and

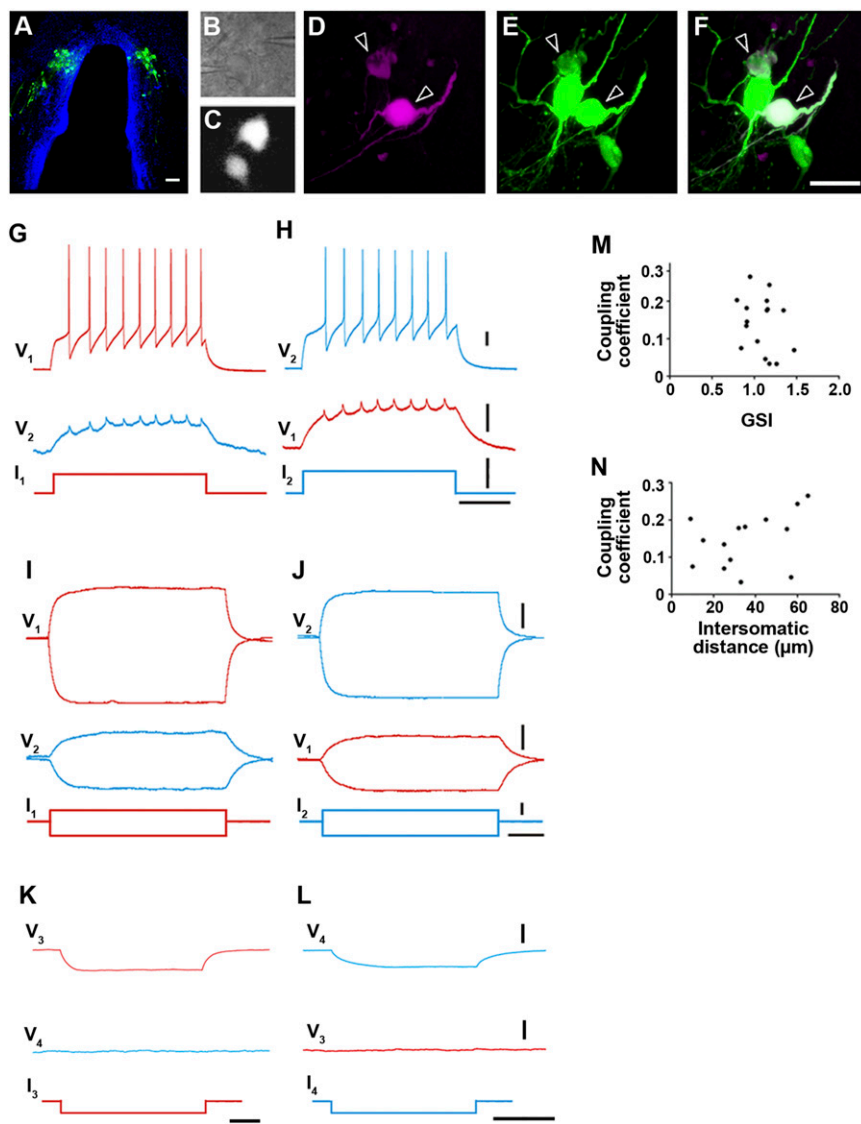


Fig. 2. GnRH1+ neurons are connected through electrical synapses. (A) Horizontal sections through the hypothalamus capture GnRH1+ cell bodies and fibers, stained for EGFP. Blue, DAPI. (B and C) Examples of recorded neurons visualized under DIC illumination (B) or with native EGFP fluorescence (C). (D–F) Detection of biocytin-filled neurons (magenta in D) after recording reveals the location of cells within the EGFP+ cell cluster (green in E and F). Arrowheads indicate the biocytin+ recorded cells. (Scale bars, 50 μ m.) (G and H) Representative paired whole-cell recordings revealing postsynaptic spikelets driven by full action potentials in presynaptic GnRH1 cells in response to suprathreshold DC current injection to either cell 1 (G) or 2 (H). (I and J) Representative paired recordings demonstrating electrical coupling with subthreshold current injection delivered to cell 1 (I) or 2 (J). (K and L) Paired recordings showing no electrical coupling between GnRH1 neurons and GnRH1-negative neurons, irrespective of which cell was stimulated. Responses are averaged passive responses to multiple current pulses in each of 4 pairs. Scale bars, voltage traces: G–J, 5 mV; K and L, 20 mV (Top) or 2 mV (Middle); current traces: 100 pA; time: 0.2 s. $n = 14$ pairs (G–J) or 3–4 pairs (K and L). (M and N) No correlation of coupling coefficient with either gonadosomatic index (M) or intersomatic distance (N) ($P \geq 0.11$, $n = 15$ –16, Pearson correlation).

Cx35 in fish). We found three homologs most closely related to mammalian *Gjd2*, which we call *Gjd2a*, *Gjd2b*, and *Gjd2c* (Fig. S5A). One of these, *Gjd2a*, appears to be a true ortholog, as the genes to the 5' end of mouse *Gjd2* (*Aqr*, *Dph6*, *Meis2*) are also found flanking *A. burtoni* *Gjd2a*. We generated antisense RNA probes against each to determine whether any was expressed in the preoptic area. We found that one of these, *Gjd2a*, was expressed in a population of large-diameter cells of the parenchyma of the preoptic area, reminiscent of GnRH1 expression (Fig. S5B). To test whether *Gjd2a* is expressed in GnRH1 neurons, we colabeled brain sections and found that $96.3 \pm 1.8\%$ of GnRH1+ neurons also express *Gjd2a* mRNA (Fig. 5; $n = 4$ fish). These results suggest that the electrical coupling we observe between GnRH1 neurons is mediated by the gap junction *Gjd2a*.

Discussion

The network we describe, formed by GnRH1 neurons in reproductively active males, comprises an essential part of the hypothalamic–pituitary–gonadal axis, the final common neural pathway regulating fertility. This discovery provides, to our knowledge, the first example of electrical synapses connecting GnRH1 neurons in a vertebrate, providing a potential mechanism for the pulsatile output required for activation of the reproductive axis. This work will allow an analysis of how this critical subset of neurons

might regulate reproductive function across vertebrates. Moreover, this report adds to the increasing recognition that gap junctions may play a larger role in vertebrate brains than had been previously recognized (32–34). Gap junctions have been detected in a variety of mammalian brain structures (23–27), as well as in fish hindbrain Mauthner cells and anterior telencephalic GnRH3 neurons that do not regulate pituitary function (35, 36).

Our results also suggest a molecular mechanism for coordinating the firing of GnRH1 neurons in *A. burtoni*. The colocalization of *Gjd2a* and *GnRH1* mRNAs indicates that this connexin is important for the electrical connection between GnRH1 neurons. We cannot rule out the possibility that other connexins may also contribute, or that presynaptic inputs could activate these neurons simultaneously. Nonetheless, the identification of *Gjd2a* provides an entrée for a genetic dissection of the basis of electrical coupling using genome modification technologies in cichlids including Tol2 and CRISPR/Cas9 (37–40). Such experiments may disentangle the respective contributions to synchrony of electrical synapses and common presynaptic inputs.

Our work raises the question of whether gap junction coupling is important for the pulsatile firing observed among GnRH1 neurons of other vertebrates including mammals. Although gap junction coupling has been observed in immortalized mouse GnRH1 neurons in cell culture (14), it has not been demonstrated in vivo. In

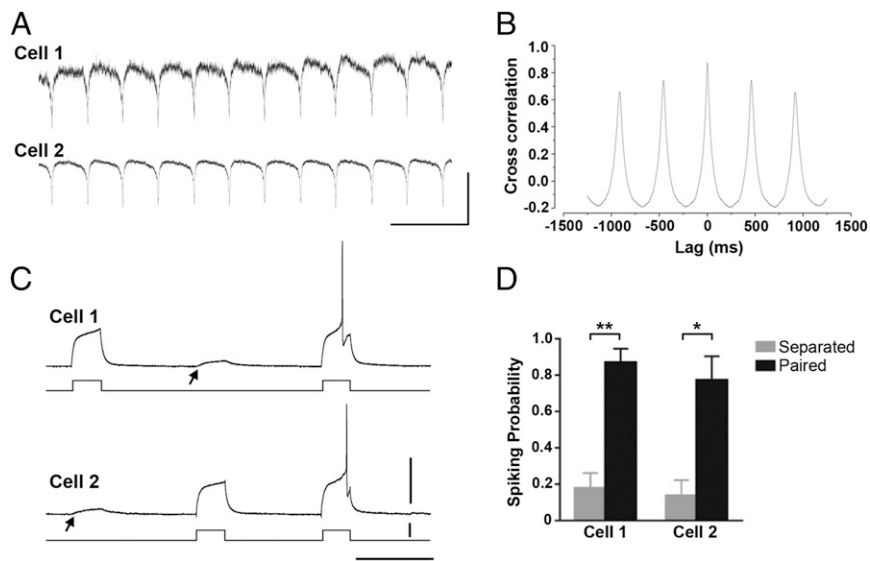


Fig. 3. GnRH1 cells exhibit synchronous spiking. (A) Example traces of two GnRH1 neurons recorded in paired voltage clamp mode in a spontaneously active slice exhibit synchronized depolarizations. (B) Cross correlation analysis of voltage-clamped responses for cells in A reveals a peak at 0 ms, consistent with network spiking synchrony. (C) A single current pulse injection in cell 1 produced no firing in either cell 1 (Upper) or cell 2 (Lower) and similarly, a single current injection in cell 2 produced no action potential in cell 2 (Lower) or cell 1 (Upper). In contrast, simultaneous current injections of the same magnitude into both cells evoked action potentials in both cells. Arrows indicate the postsynaptic membrane depolarization induced by current injection into presynaptic cells. (D) Simultaneous current injection enhances spiking probability. * $P = 0.02$, ** $P = 0.004$; paired t test; $n = 7$ pairs of neurons; mean \pm SEM. (Scale bars: 100 pA, 1 s in A; 40 mV in voltage traces in C, 200 pA for current traces in C; time scale bar, 0.4 s.)

the mouse, paired recordings in GnRH1 neurons have found very low rates of electrical coupling (17, 41), and microscopic reconstructions have not reproducibly shown pairing between GnRH1 neurons (16). This difference from the cichlid has at least two possible explanations. First, gap junctions may connect GnRH1 neurons in mammals, but be rarely detected for biological or technical reasons. Although *Gjd2* and *Gja1* were not found in mouse GnRH1 neurons, another member of the connexin gene family is likely present, as these neurons pass dyes to neighboring, non-GnRH1 cells (17). It is possible that the use of dominant male *A. burtoni*, which are continuously reproductively active (21), improved our chances of detecting electrical coupling. Electrical synapse strength is known to be dynamically regulated by many factors including the activity of chemical synapses and neuromodulators (32). Thus, it is possible that during recordings from mouse GnRH1 neurons, dye transfer and/or electrical coupling was precluded by gap junction inhibition. An alternative explanation is that the presence of gap junction coupling in the cichlid represents a species difference. In this scenario, gap junction coupling between GnRH1 neurons is one of multiple solutions that the neuroendocrine axis may use to facilitate pulsatile activation of the pituitary, and the evolutionary lineage leading to mice employs a different solution than cichlids. Future work on a variety of organisms will address whether electrical coupling among GnRH1 neurons is an ancestral trait, and may reveal mechanisms shared across vertebrates that coordinate pulsatile GnRH1 delivery.

Materials and Methods

GnRH1:EGFP Transgene Construction. To label cichlid GnRH1 neurons, we used regulatory elements from the *A. burtoni* GnRH1 locus to drive EGFP expression in those cells. We PCR amplified a 5,202-bp region 5' from the endogenous GnRH1 start codon, which included 5,039 kb 5' of the transcription start site, plus noncoding sequence from the first exon and intron, and 13 bp of exon 2 preceding the start codon. We also amplified 689 bp of sequence following the translational stop, including the *GnRH1* 3' UTR. These sequences were inserted, along with EGFP, into a modified pT2-KXIG Δ in plasmid (42) containing Tol2 transposase recognition sites flanking an XhoI-PacI-BamHI-EcoRV-AscI-BglII polylinker, to create the pT2-GnRH1:EGFP plasmid. All amplified sequences were confirmed using Sanger sequencing (ElimBio). The pT2-GnRH1:EGFP plasmid was purified by maxiprep (Qiagen).

Animals. All experiments were conducted according to the protocols approved by the Stanford Institutional Animal Care and Use Committee. For transgenic fish production, wild-type fish were housed separately by sex, separated by a partition. On the day of injection, the partition was removed, and females were allowed to spawn with a male. Fertilized eggs were collected ~30 min after spawning, and injected during the single-cell stage (40) with ~1 nL of a mixture containing pT2-GnRH1:EGFP (225 ng/ μ L), *Tol2* mRNA transcribed

from pCS-TP (43) (225 ng/ μ L), and Texas Red-conjugated dextran (0.5%; 3000 MW; Sigma) for visualization of injection. Each injected egg was allowed to develop alone in a well of a 6-well culture dish (Greiner Bio-One) with each well containing 6 mL of tank water supplemented with 1 mg/L methylene blue antifungal (Sigma). At ~12 d postfertilization (dpf), injected larvae were transferred to 1.5-L tanks, and then to 32-L tanks at ~4 wk of age.

A total of 137 out of 369 injected single cell eggs developed normally to ~12 d of age and carried the Texas Red injection marker. As EGFP expression was not visible in *A. burtoni* at 14 dpf, the day of GnRH1 onset (44), 75 of these injected fish were cohoused and their offspring were screened by PCR for germ-line transmission of the *GnRH1:EGFP* transgene using PCR as follows. When F₁ fry were large enough to collect fin clips (~5 wk post-fertilization), a small tissue sample was obtained from the tailfin of each fry, and DNA was extracted in a 15 min incubation in 50 mM NaOH at 95 °C and neutralization with 1 M Tris (pH 8.0) (45). F₁ carriers of the *GnRH1:EGFP* transgene were identified through PCR with the primers GnRH1genoFwd (5'-GCA GCA GAC TTC ACA AAG GAC AG-3') and EGFPgenoRev (5'-AGC TTG CCG TAG GTG GCA TC-3'). Two male F₀ founder fish were identified that passed the *GnRH1:EGFP* transgene to offspring, and were able to successfully propagate one line with robust GFP fluorescence. A hemizygous F₁ *GnRH1:EGFP*+ male was bred with wild-type females to generate fish used in this study. PCR confirmed that 55% of genotyped F₂ fish carried the *GnRH1:EGFP* transgene ($n = 165$ fish), consistent with a single autosomal insertion.

F₂ *GnRH1:EGFP*+ fish at 5–7 mo of age were group-housed with their siblings in 32-L tanks, each housing 3–4 males and 3–4 females. Dominance was confirmed through behavioral observation of male-typical reproductive and dominance behaviors (46) before their terminal use for electrophysiological recordings. Reproductive status was confirmed by measuring the gonadosomatic index (Gonad mass/body mass \times 100), which was 1.04 ± 0.5 ($n = 18$), in the range observed for dominant animals (4).

Connexin Gene Identification. We used connexin 35/36 (mouse, NP_034420; perch, AAC_31884.1) and connexin 43 (mouse, NP_034418.1) protein sequences to identify connexins in the *A. burtoni* genome with a tBLASTn search (47). We identified 26 putative connexins, which we assembled using Geneious (Biomatters v7.1; MUSCLE alignment, Jukes-Cantor end-joining, 1,000 bootstrap replicates) into a phylogenetic tree along with other refseq connexin protein sequences identified from vertebrate species. The three genes that clustered with *Gjd2* we refer to as *Gjd2a* (XP_005942712, encoded by XM_005942650), *Gjd2b* (splice variants XP_005922104 and XP_005922105, encoded by XM_005922042 and XM_005922043), and *Gjd2c* (XP_005926648, encoded by XM_005926586). Other vertebrate connexin accession numbers are reported in Table S2.

In Situ Hybridization. *Gjd2* probes were synthesized using PCR to amplify from hypothalamus cDNA, in which the 3' probe contained a T7 polymerase binding site, enabling transcription of antisense RNA from PCR product. *Gjd2a* forward, 5'-AGA GAC GAG GAC GGT AGC AG-3'; *Gjd2a* reverse, 5'-GAA ATT AAT ACG ACT CAC TAT AGG GCT TGC CTC CTC ATT TTG GAC-3';

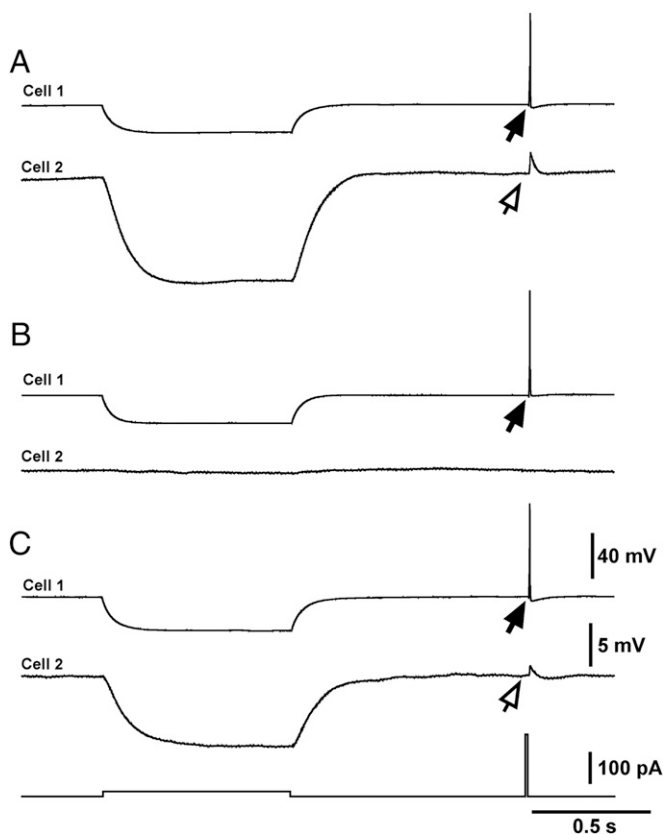


Fig. 4. Electrical synapses between GnRH1 cells are blocked by meclofenamic acid. (A) Control sweeps demonstrate electrical coupling at sub-threshold and suprathreshold conditions. (B) Nearly complete blockade of electrical coupling by meclofenamic acid (400 μ M; after 30 min). (C) Recovery after washout (45 min). Filled and open arrows mark a presynaptic action potential and the postsynaptic membrane response, respectively. $n = 4$.

Gjd2b forward, 5'-GAG GGG AAG GAG AAC AGA GG-3'; Gjd2b reverse, 5'-GAA ATT AAT ACG ACT CAC TAT AGG GAG TAG CGG ATG TGC GAG ATT-3'; Gjd2c forward, 5'-CGA TGG ATG TCT GTT TGC AC-3'; Gjd2c reverse, 5'-GAA ATT AAT ACG ACT CAC TAT AGG GCA TAG CAA GCT TGG TTG CAG-3'. T7 polymerase binding sites are underlined. The *Gjd2b* probe was designed to detect a region common to both splice isoforms. The *GnRH1* probe was transcribed from a pCRII-TOPO plasmid containing bp 11–206 of *GnRH1* cDNA (NM_001286296.1).

Brains were processed and sectioned as for immunohistochemistry, except that brains were fixed in PFA with pH 7.0. Sections were fixed on slides with PFA, proteinase K treated for 15 min, and fixed again. We acetylated sections before incubating overnight at 60 $^{\circ}$ C in hybridization buffer containing 0.2 ng/mL of antisense RNA probes labeled with fluorescein (*GnRH1*) and/or digoxigenin (*Gjd2a*). Sections were washed the following day in a series of washes containing 50% formamide + 2 \times SSC, 2 \times SSC (one wash containing RNase A, 0.2 μ g/mL), and then maleic acid buffer plus 0.1% Tween-20 (MABT; for nonfluorescent stain) or Tris-buffered saline plus 0.1% Tween-20 (TNT; for fluorescent stain). Sections were blocked in MABT containing BSA [nonfluorescent stain, 2% (wt/vol)] or in TNT containing blocking reagent (double fluorescent

stain, Roche, 0.5%). Antisense probes were detected using horseradish peroxidase-coupled anti-fluorescein or alkaline phosphatase-coupled anti-digoxigenin Fab fragments (Roche) incubated overnight at 4 $^{\circ}$ C. Unbound antibody was washed using MABT or TNT, and then alkaline phosphatase was detected using NBT and BCIP (nonfluorescent stain; Roche) or HnPP/Texas Red (fluorescent stain; Roche) for 3 h. For fluorescent staining, excess HnPP was washed away with TNT, and then *GnRH1* was detected using a TSA-fluorescein signal amplification kit (Perkin-Elmer) for 20 min. Extended protocol available upon request.

Immunohistochemistry. To confirm that EGFP was expressed in the same cell population as GnRH1, we immunostained cryosections of brain with antibodies against EGFP and GnRH1. F₂ *GnRH1:EGFP* fish were dissected, brains were fixed overnight in 4% paraformaldehyde (PFA), then cryoprotected with 30% sucrose in 0.1 M PBS overnight. Brains were embedded in Neg 50 (Thermo), and stored at -80° C until they were cryosectioned into 30 μ m sections onto two alternate sets of slides. Cells were counted on only one set of slides to preclude double-counting of cells on subsequent sections. Slides were washed in 0.1 M PBS plus 0.1% Triton X-100 (PT), incubated in PT plus 5% normal goat serum (Life Technologies) to block nonspecific staining, and stained overnight at 4 $^{\circ}$ C with mouse anti-EGFP (1:500; Life Technologies) and guinea pig anti-GnRH1 in PT plus 0.5% goat serum. Custom anti-GnRH1 antibody was raised against cichlid mature GnRH1 decapeptide (QHWSYGLSPG; Thermo). Sections were washed in PT plus 0.5% goat serum. Secondary antibodies Alexa488-conjugated goat anti-mouse and Texas Red-conjugated goat anti-guinea pig (Jackson ImmunoResearch) were used to detect primary antibodies.

To visualize cells recorded electrophysiologically, neurons were filled with 0.2% biocytin (Sigma) during recording. Slices were fixed overnight in 4% PFA, washed with PBS, and then immunostained with mouse anti-EGFP and Texas Red-conjugated Avidin D (1:100; Vector Laboratories) in PBS plus 1% Triton X-100 and 0.5% goat serum.

To image stained sections, we used a Zeiss LSM 700 confocal microscope with optical section thickness of 2 μ m and pinhole size of 1 to capture the entire extent of staining in a Z-stack. AlexaFluor-488 and Texas Red filters were used to image fluorophores. Images were despeckled using ImageJ (NIH). For colocalization studies, each cell labeled for EGFP or GnRH1 was enumerated, and scored for the presence of the other epitope; for in situ hybridization, all *GnRH1*-positive cells were scored for the presence of *Gjd2a*.

Electrophysiological Slice Preparation. Five- to 7-mo-old transgenic fish were weighed, standard body length measured, and rapidly decapitated. Brains were carefully taken out of the skull and placed in a Petri dish filled with ice-cold slicing solution containing 234 mM sucrose, 11 mM D-glucose, 2.5 mM KCl, 1.25 mM NaH₂PO₄, 0.5 mM CaCl₂, 2.0 mM MgSO₄, and 26 mM NaHCO₃. Optic nerves and attached meninges were gently trimmed. Then the brain was placed into 4% low melting point agarose (30–35 $^{\circ}$ C) in a small plastic chamber. The preoptic area (POA) was gently positioned to obtain the slicing angle as described previously, orienting the brain to cut parallel to the ventral surface just above the GnRH1 neurons. This orientation is most suitable for electrophysiological recordings of GnRH1 neurons because they lie roughly in a plane parallel to the ventral brain surface (28). The agarose block containing the fish brain was quickly cooled, trimmed and mounted onto a vibratome (VT1200, Leica Microsystems). The tissue above the POA was eliminated by lowering the slicing blade in small steps until the EGFP in the POA was visible. Then one or two slices (250 μ m thickness) containing POA were sectioned, transferred and incubated at room temperature in ACSF solution containing 126 mM NaCl, 2.5 mM KCl, 1.25 mM NaH₂PO₄, 2.0 mM CaCl₂, 2.0 mM MgSO₄, 26 mM NaHCO₃, 10 mM D-glucose, bubbled with 95% O₂/5% CO₂. At the end of the slicing procedure, gonads were dissected and weighed to calculate the gonadosomatic index.

Electrophysiological Recordings. After at least 1 h of incubation, slices were transferred into a recording chamber mounted on an upright Zeiss microscope

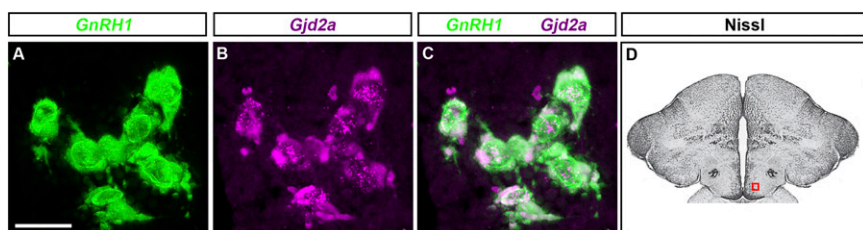


Fig. 5. GnRH1 neurons express mRNA for the connexin *Gjd2a*. POA sections were fluorescently labeled for mRNA encoding *GnRH1* (A) and *Gjd2a* (B); merged channels are shown in C. Nissl-stained section highlights region displayed (D). (Scale bar, 30 μ m in A–C.)

equipped with a 40× water immersion Zeiss objective and a Hamamatsu CCD camera (model C2400-75). EGFP+ cells in the POA were identified by epifluorescence illumination (X-Cite series 120Q; EGFP filter cube, Chroma), controlled by a Uniblitz shutter and driver (model VMM-D1, Vincent Associates). Patch pipettes (tip resistance 4–7 MΩ) were pulled from borosilicate glass capillaries (O.D./I.D., 1.5/1.1 mm, Sutter Instruments) and back-filled with internal solutions containing 135 mM K-gluconate, 7 mM KCl, 10 mM Hepes, 1.1 mM EGTA, 4 mM ATP-Mg, 6 mM phosphocreatine, 0.2% biocytin (pH 7.25–7.35, osmolarity 280–290 mOsm). Simultaneous whole-cell recording from pairs of neurons was performed with continuous perfusion of oxygenated ACSF at a rate of 2–3 mL/min at 23–27 °C using MultiClamp 700A and Digidata 1440A (Molecular Devices) with a filter of 10 kHz and sampling rate of 20–100 kHz. Measures of passive membrane properties of GnRH1 neurons (Table S1) were consistent to those previously found (28). We recorded from 18 pairs of transgenically labeled GnRH1 neurons with intersomatic distances ranging from 15 to 65 μm, (mean = 35 μm) in the POA of brain slices.

First, a gigohm seal, cell-attached recording was made with one labeled GnRH1 cell and spontaneous neuronal activity was recorded in voltage-clamp mode with a holding voltage of –60 mV for 2–4 min. After membrane break-in to establish whole-cell recording mode, passive and active membrane properties were assessed with short pulses of DC current injection using conventional techniques. Then the same procedure was followed for a second cell, including characterization of its electrical properties.

- Phoenix CH, Goy RW, Gerall AA, Young WC (1959) Organizing action of prenatally administered testosterone propionate on the tissues mediating mating behavior in the female guinea pig. *Endocrinology* 65:369–382.
- Morris JA, Jordan CL, Breedlove SM (2004) Sexual differentiation of the vertebrate nervous system. *Nat Neurosci* 7(10):1034–1039.
- Forni PE, Wray S (2014) GnRH, anosmia and hypogonadotropic hypogonadism - Where are we? *Front Neuroendocrinol* 36C:165–177.
- Davis MR, Fernald RD (1990) Social control of neuronal soma size. *J Neurobiol* 21(8):1180–1188.
- Wierman ME, Kiseljak-Vassiliades K, Tobet S (2011) Gonadotropin-releasing hormone (GnRH) neuron migration: initiation, maintenance and cessation as critical steps to ensure normal reproductive function. *Front Neuroendocrinol* 32(1):43–52.
- Schwanzel-Fukuda M, Pfaff DW (1989) Origin of luteinizing hormone-releasing hormone neurons. *Nature* 338(6211):161–164.
- Moenter SM (2010) Identified GnRH neuron electrophysiology: a decade of study. *Brain Res* 1364:10–24.
- Belchetz PE, Plant TM, Nakai Y, Keogh EJ, Knobil E (1978) Hypophysial responses to continuous and intermittent delivery of hypothalamic gonadotropin-releasing hormone. *Science* 202(4368):631–633.
- Karigo T, et al. (2014) Whole brain-pituitary in vitro preparation of the transgenic medaka (*Oryzias latipes*) as a tool for analyzing the differential regulatory mechanisms of LH and FSH release. *Endocrinology* 155(2):536–547.
- Krsmanovic LZ, Hu L, Leung PK, Feng H, Catt KJ (2009) The hypothalamic GnRH pulse generator: multiple regulatory mechanisms. *Trends Endocrinol Metab* 20(8):402–408.
- Tsutsumi R, Webster NJ (2009) GnRH pulsatility, the pituitary response and reproductive dysfunction. *Endocr J* 56(6):729–737.
- Habibi HR (1991) Homologous desensitization of gonadotropin-releasing hormone (GnRH) receptors in the goldfish pituitary: effects of native GnRH peptides and a synthetic GnRH antagonist. *Biol Reprod* 44(2):275–283.
- Richter TA, Keen KL, Terasawa E (2002) Synchronization of Ca(2+) oscillations among primate LHRH neurons and nonneuronal cells in vitro. *J Neurophysiol* 88(3):1559–1567.
- Bose S, Leclerc GM, Vasquez-Martinez R, Boockfor FR (2010) Administration of connexin43 siRNA abolishes secretory pulse synchronization in GnRH clonal cell populations. *Mol Cell Endocrinol* 314(1):75–83.
- Vazquez-Martinez R, Shorte SL, Boockfor FR, Frawley LS (2001) Synchronized exocytotic bursts from gonadotropin-releasing hormone-expressing cells: dual control by intrinsic cellular pulsatility and gap junctional communication. *Endocrinology* 142(5):2095–2101.
- Campbell RE, Gaidamaka G, Han SK, Herbison AE (2009) Dendro-dendritic bundling and shared synapses between gonadotropin-releasing hormone neurons. *Proc Natl Acad Sci USA* 106(26):10835–10840.
- Campbell RE, et al. (2011) Gap junctions between neuronal inputs but not gonadotropin-releasing hormone neurons control estrous cycles in the mouse. *Endocrinology* 152(6):2290–2301.
- White SA, Kasten TL, Bond CT, Adelman JP, Fernald RD (1995) Three gonadotropin-releasing hormone genes in one organism suggest novel roles for an ancient peptide. *Proc Natl Acad Sci USA* 92(18):8363–8367.
- White SA, Fernald RD (1993) Gonadotropin-releasing hormone-containing neurons change size with reproductive state in female *Haplochromis burtoni*. *J Neurosci* 13(2):434–441.
- Francis RC, Soma K, Fernald RD (1993) Social regulation of the brain-pituitary-gonadal axis. *Proc Natl Acad Sci USA* 90(16):7794–7798.
- Fernald RD, Maruska KP (2012) Social information changes the brain. *Proc Natl Acad Sci USA* 109(Suppl 2):17194–17199.
- Kawakami K (2007) Tol2: a versatile gene transfer vector in vertebrates. *Genome Biol* 8(Suppl 1):S7.
- Zsiros V, Maccaferri G (2008) Noradrenergic modulation of electrical coupling in GABAergic networks of the hippocampus. *J Neurosci* 28(8):1804–1815.
- Lee SC, Patrick SL, Richardson KA, Connors BW (2014) Two functionally distinct networks of gap junction-coupled inhibitory neurons in the thalamic reticular nucleus. *J Neurosci* 34(39):13170–13182.
- Wang Y, Barakat A, Zhou H (2010) Electrotonic coupling between pyramidal neurons in the neocortex. *PLoS ONE* 5(4):e10253.
- Gibson JR, Beierlein M, Connors BW (1999) Two networks of electrically coupled inhibitory neurons in neocortex. *Nature* 402(6757):75–79.
- Galarreta M, Hestrin S (1999) A network of fast-spiking cells in the neocortex connected by electrical synapses. *Nature* 402(6757):72–75.
- Greenwood AK, Fernald RD (2004) Social regulation of the electrical properties of gonadotropin-releasing hormone neurons in a cichlid fish (*Astatotilapia burtoni*). *Biol Reprod* 71(3):909–918.
- Bennett MV, Zukin RS (2004) Electrical coupling and neuronal synchronization in the mammalian brain. *Neuron* 41(4):495–511.
- Veruki ML, Hartveit E (2009) Meclofenamic acid blocks electrical synapses of retinal All amacrine and on-cone bipolar cells. *J Neurophysiol* 101(5):2339–2347.
- Harks EG, et al. (2001) Fenamates: a novel class of reversible gap junction blockers. *J Pharmacol Exp Ther* 298(3):1033–1041.
- Pereda AE (2014) Electrical synapses and their functional interactions with chemical synapses. *Nat Rev Neurosci* 15(4):250–263.
- Levavi-Sivan B, Bloch CL, Gutnick MJ, Fleidervish IA (2005) Electrotonic coupling in the anterior pituitary of a teleost fish. *Endocrinology* 146(3):1048–1052.
- Söhl G, Maxeiner S, Willecke K (2005) Expression and functions of neuronal gap junctions. *Nat Rev Neurosci* 6(3):191–200.
- Pereda AE, Bell TD, Faber DS (1995) Retrograde synaptic communication via gap junctions coupling auditory afferents to the Mauthner cell. *J Neurosci* 15(9):5943–5955.
- Haneda K, Oka Y (2008) Coordinated synchronization in the electrically coupled network of terminal nerve gonadotropin-releasing hormone neurons as demonstrated by double patch-clamp study. *Endocrinology* 149(7):3540–3548.
- Li M, et al. (2014) Efficient and heritable gene targeting in tilapia by CRISPR/Cas9. *Genetics* 197(2):591–599.
- Doudna JA, Charpentier E (2014) Genome editing. The new frontier of genome engineering with CRISPR-Cas9. *Science* 346(6213):1258096.
- Hwang WY, et al. (2013) Efficient genome editing in zebrafish using a CRISPR-Cas system. *Nat Biotechnol* 31(3):227–229.
- Juntti SA, Hu CK, Fernald RD (2013) Tol2-mediated generation of a transgenic haplochromine cichlid, *Astatotilapia burtoni*. *PLoS ONE* 8(10):e77647.
- Suter KJ, Wuari JP, Smith BN, Dudek FE, Moenter SM (2000) Whole-cell recordings from preoptichthalamal slices reveal burst firing in gonadotropin-releasing hormone neurons identified with green fluorescent protein in transgenic mice. *Endocrinology* 141(10):3731–3736.
- Urasaki A, Morvan G, Kawakami K (2006) Functional dissection of the Tol2 transposable element identified the minimal cis-sequence and a highly repetitive sequence in the subterminal region essential for transposition. *Genetics* 174(2):639–649.
- Kawakami K, et al. (2004) A transposon-mediated gene trap approach identifies developmentally regulated genes in zebrafish. *Dev Cell* 7(1):133–144.
- White RB, Fernald RD (1998) Ontogeny of gonadotropin-releasing hormone (GnRH) gene expression reveals a distinct origin for GnRH-containing neurons in the mid-brain. *Gen Comp Endocrinol* 112(3):322–329.
- Meeker ND, Hutchinson SA, Ho L, Trede NS (2007) Method for isolation of PCR-ready genomic DNA from zebrafish tissues. *Biotechniques* 43(5):610, 612, 614.
- Fernald RD, Hirata NR (1977) Field-Study of Haplochromis-Burtoni - Quantitative Behavioral Observations. *Anim Behav* 25(Nov):964–975.
- Altschul SF, et al. (1997) Gapped BLAST and PSI-BLAST: a new generation of protein database search programs. *Nucleic Acids Res* 25(17):3389–3402.